01 Mar 2022

Selective Penetration Behavior of Microgels in Superpermeable Channels and Reservoir Matrices

Yang Zhao

Baojun Bai
Missouri University of Science and Technology, baib@mst.edu

Journal of Petroleum Science and Engineering 210 (2022) 109897

Contents lists available at ScienceDirect

Journal of Petroleum Science and Engineering

journal homepage: www.elsevier.com/locate/petrol

Selective penetration behavior of microgels in superpermeable channels and reservoir matrices

Yang Zhao, Baojun Bai [*]

Department of Geosciences and Geological and Petroleum Engineering, Missouri University of Science and Technology, 1400 N Bishop Ave, Rolla, MO, 65409, United States

A R T I C L E I N F O

Keywords:
Enhanced oil recovery
Conformance control
Gel treatment
Preformed particle gel
Threshold penetration pressure

A B S T R A C T

Gel treatment is an effective way to attack excessive water production in many mature oilfields around the world. Selective penetration is desired for successful gel treatments. That is, gel materials should easily penetrate the target zones (i.e., channeling features such as superpermeable channels) without entering/damaging the nontarget zones (i.e., reservoir matrices or oil zones). This study revealed that presence of threshold penetration pressure (ΔP_{th}) was responsible for selective penetration behavior of tested microgels. The concept of ΔP_{th} was utilized to figure out favorable working conditions for effective gel treatments. Microgel dispersions were injected into superpermeable (super-k) sandpacks (mimicking super-k channels in reservoirs, 60–221 darcies), heterogeneous models with super-k channels (79–230 darcies), and sandstone cores (mimicking reservoir matrices, 50–5000 md). The results demonstrated that a minimum differential driving pressure (i.e., threshold penetration pressure, ΔP_{th}) was required to push microgel particles to penetrate channels or matrices. The critical penetration behavior was closely related to the particle/pore size ratio. Low ΔP_{th} at smaller particle/pore ratios was beneficial to allow easy penetration of gel materials into the channeling zones. On the contrary, high ΔP_{th} at larger particle/pore ratios was desirable to prevent gel materials from massively invading and damaging the matrices. Instead, the gel particles accumulated at the inlet surface, and a gel cake was gradually formed. The cake further prevented the invasion of the gels. The cake could be removed by chemical breakers to resume the injectivity/productivity of the matrices. Correlations were developed to describe the relationship between ΔP_{th} and particle/pore ratio. A distinct transition was identified at the particle/pore ratio of about 3. This work could help identify the favorable conditions to achieve successful gel treatments. In an effective conformance treatment, the particle/pore ratio in the channel should be sufficiently low to allow easy penetration of gel materials into the channel (e.g., particle/pore ratio$<$2 in this study). Meanwhile, the particle/pore ratio in the matrix should be large enough to support a high ΔP_{th} and thus prevent massive gel invasion into the matrix. This study advances the current pore scale studies (a single particle passing through a single channel) to Darcy-scale characterization.

1. Introduction

Excessive water production is a big challenge and is commonly encountered in oil fields around the world. Fractures and fracture-like features present in reservoirs are among the major reasons that responsible for the excessive water production. As illustrated in Fig. 1a, flooding fluids (water, polymer solution, etc.) would channel through the super-k channels, leaving a large portion of oil in the matrices unswept. Gel treatment has been proven effective to block fractures and fracture-like features in reservoirs and improve the conformance. Different gel products have been developed over the last several decades (Seright and Brattekas, 2021; Leng et al., 2021; Zhu et al., 2017; Kang et al., 2021; Choi et al., 2013), such as in-situ gels (Sydansk and Romero-Zeron, 2011; Bai et al., 2021), preformed bulk gels (Seright, 1997), and preformed particle gels (Bai et al. 2007a, 2008, 2012, 2013; Esfahlan et al., 2021). Each gel system has its own unique characteristics and advantages (e.g., thermal stability, tolerance to high salinity, thermal-responsive ability, pH-responsive feature, strength, injectivity, etc.) to accommodate different reservoir situations (e.g., sources of excessive water production, channeling types, temperature, salinity,

* Corresponding author.
E-mail address: baib@mst.edu (B. Bai).

https://doi.org/10.1016/j.petrol.2021.109897
Received 29 July 2021; Received in revised form 25 October 2021; Accepted 21 November 2021
Available online 23 November 2021

well types, well completion conditions, etc.) (Seright and Brattekas, 2021; Zhu et al., 2017; Choi et al., 2013; Koochakzadeh et al., 2021; Lalehrokh and Bryant, 2009; Teimouri et al., 2020; Leng et al., 2021).

The target reservoir is located in Milne Point Unit on Alaska's North Slope (ANS). The first-ever polymer flooding project on ANS has been ongoing since August 2018 to develop the abundant heavy oil resources (Dandekar et al. 2019, 2020, 2021; Ning et al., 2020). Conformance control is an important aspect to ensure the success of polymer flooding in heavy oil reservoirs, especially when channeling features are present in the reservoirs (Zhao et al., 2021b). Production responses and field-scale reservoir simulation studies indicated presence of high-permeability streaks in the target reservoir. No satisfactory history matching could be achieved by adjusting input parameters within reasonable ranges, such as relative permeabilities, residual oil saturation, skin factors, etc. Presence of open fractures was ruled out based on flooding performance and inter-well chemical tracer tests before and after implementation of polymer flooding. The project team (including the operator, universities and consultants) proposed that high-permeability streaks (not fractures) were very likely in the reservoir. Production behavior after polymer flooding supported this speculation. Inter-well chemical tracer tests before and after implementation of the polymer flooding also supported (at least did not deny) this possibility. Follow-up simulation work demonstrated that good history matching was established after introducing some high-permeability streaks (i.e., superpermeable porous channels) into the reservoir (Wang et al., 2021). As high as ~200 darcies was tested in the history match studies. In view of the highly possible high-permeability streaks, conformance treatment laboratory studies were carried out to explore effective ways and materials to deal with these super-k channels. Our previous experimental studies suggested that micron-sized preformed particle gels (microgels) could improve the effectiveness of polymer flooding when superpermeable channels were present in reservoirs (Zhao et al., 2021b). This work intended to further explore the critical penetration conditions and favorable working conditions for successful microgel treatments.

As for the occurrence of such high-permeability streaks in reservoirs, sand mobilization and production (flow conditions) may play a role as the reservoir is weakly-consolidated or even unconsolidated (weak geological/sedimentary conditions) (Dandekar et al., 2019). Wormholes can be induced as the oil in place is produced and the reservoir pressure is reduced. Therefore, high-permeability streaks can be gradually generated (Mathur et al., 2017). Such streaks may also exist in reservoirs with similar geological/sedimentary conditions, such as the Ugnu heavy oil on ANS (Mathur et al., 2017).

Selective penetration of gel materials is desired for successful gel treatments. That is, the gel materials should easily penetrate the target zones (i.e., the channeling features such as super-k channels) without entering/damaging the nontarget zones (i.e., the matrices or oil zones). In an effective gel treatment, as shown in Fig. 1b, the gel materials are expected to efficiently shut off the super-k features, and thus the subsequent flooding fluid can be diverted to the matrices to displace the remaining oil previously left behind (Zhao et al., 2021b). For particulate gels, some researchers have studied the driving pressures that are required to push the viscoelastic particles to transport through pore throats at different scales. Pore-scale experimental studies (Bai et al., 2007b; Yao et al. 2014, 2020; Wang et al., 2017; Zhao et al., 2018) and numerical studies (Liu et al., 2017; Zhou et al., 2017; Lei et al., 2019) shed light on the understanding of the transport, plugging, and remigration behaviors of viscoelastic particles through pore-throat structures. Besides, studies outside the oil industry also provide insights to the transport mechanisms of microgel particles through microchannels analogous to a pore throat. Interested readers are encouraged to reach the following articles as a start for more information: Hendrickson and Lyon (2010), Zhang et al. (2018) and Villone and Maffettone (2019).

The resistance forces applied on a gel particle include structural forces by pore-throat walls, and frictional forces by pore-throat surfaces, while the driving force is from drag of the carrying fluid. When a gel particle is larger than the pore throat, additional forces are required to make it deform in order to pass through the throat. The maximum resistance is believed to occur as the particle right in the middle of the throat (narrowest spot) (Yao et al., 2014; Wang et al., 2017; Zhao et al., 2018). Therefore, a minimum differential driving pressure is required to make the particle deform and overcome the maximum resistance. Thus, the particle can pass through the throat. Different terms are used to denote this minimum differential pressure, e.g., critical pressure (Lei et al., 2019), threshold pressure (Wang et al., 2017), restarting pressure (Zhao et al., 2018) and remigration pressure (Yao et al., 2014). In our work, the term threshold pressure (ΔP_{th}) is adopted. Below the threshold pressure, the gel particle will be entrapped at pore throat and cannot transport downstream. This behavior is desired in low-permeability zones (oil zones). In these zones, the threshold pressure should be sufficiently high to prevent gel materials invading or damaging the oil zones. On the other hand, the threshold pressure in the channeling zones should be practically low to allow smooth injectivity and migration of the gel materials. Thus, the threshold penetration pressure is an important parameter to determine the effectiveness of gel treatments.

In the literature, the critical migration condition is also described with the concept of critical pressure gradient, which is practically more meaningful. On the core- or reservoir-scale, a gel particle dispersion is injected into a medium with multiple pore throats, rather than a single/dispersed particle through a single pore throat. The transport behavior is a result of the statistical average of groups of particles behavior and their interactions. Bai et al. (2007b) reported that the pressure gradient increased with the strength and the diameter ratio of the particle to the pore throat size. For weak particles (moderately deformable flowing gel through a tube), the break-and-pass pattern would occur when the pressure gradient exceeded a critical value. Deform and pass pattern of microspheres through pore throats was observed by Yao et al. (2014). When a sufficient driving pressure gradient was available, the microspheres would deform and change its shape to an ellipsoid, and then pass the throat. Afterwards, the particles would quickly recover most of their original shape and size. Li et al. (2015) investigated the transport

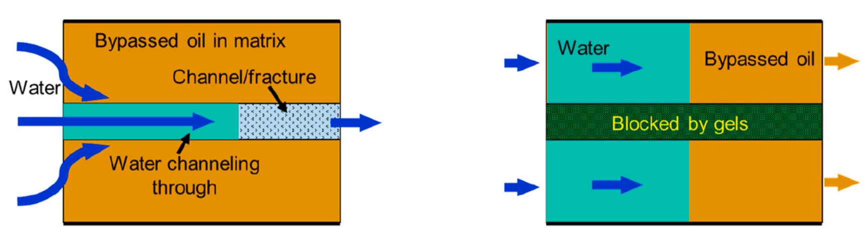

(a) A superpermeable channel is present in the reservoir. (b) The channel is shut off with gels.

Fig. 1. Gel treatment to reduce the unwanted water production and improve the effective sweep volume. [(a) A superpermeable channel or open fracture is present in the reservoir. Water, polymer, or other flooding fluids flow through the super-k channels. The oil in the matrices is bypassed. (b) The channel is shut off with gels. The subsequent flooding fluids are forced into the matrices to displace the bypassed oil.].

behavior of a single hydrogel particle through a single narrow capillary with a constriction. Their study suggests that the differential driving pressure, and the dehydration degree (volume shrinkage) depended only on the confinement degree (i.e., particle/capillary size ratio) and the geometry of tapered region. They were independent of the strength (composition) of the particles, and they were also independent of the composition of the particles or the solvent. Saghafi et al. (2016) studied the effect of various flow characteristics and properties of micron-sized preformed particle gels (37–105 μm) on resistance factors and residual resistance factors in high permeability carbonate porous media (58–395 darcies). They observed that the injection pressure increased with particle/pore size ratio. The increase was gradual as the size ratio was below 1.8 and was more drastic above 1.8. The behavior was believed a result of different dominant transport patterns at different size ratio conditions. Wang et al. (2017) studied the transport behavior of gel particles using a capillary tube with a convergent-divergent structure. The gel particles they used were relatively strong (2.2, 4.8, and 6.4 kPa), and the diameter was about 1 mm. As later reported by Zhao et al. (2018), the maximum pressure drop across the capillary model was regarded as the threshold pressure [termed as restarting pressure in their subsequent work by Zhao et al. (2018)]. The superficial velocity was quite high at the throat in their experiments (~60 ft/d at the throat). They investigated the impact of particle size, pore size, particle strength, frictional coefficient, and Poisson's ratio on the restarting pressure. Lei et al. (2019) reported a power-law relationship between the critical differential pressure (i.e., ΔP_{th}) and the elastic modulus (Young's modulus) and the particle/throat size ratio. Farasat et al. (2021) performed experimental and numerical studies of preformed particle gels in mature waterflooded reservoirs. They recommended a particle/pore size ratio of 1.75 to allow both easy propagation and low washing out of the particle gels. Esfahlan et al. (2021) summarized the progresses and future opportunities of researches and field applications of preformed particle gels. With a comprehensive review of simulation studies of preformed particle gels in fractures and porous media at different scales, Leng et al. (2021) pointed out important considerations in the simulation of preformed particle gels transport behaviors at different scales.

The brief literature review indicates that the existing studies on the critical penetration conditions are mainly focused on pore scale processes. The achievements are helpful for understanding the transport mechanisms. However, inter-particle interactions are usually overlooked or ruled out in pore scale studies. At core scale or field scale, however, interparticle interactions are significant when injecting gel suspensions, especially at high concentration conditions. The results of pore-scale studies are hard to scale up. There are seldom studies so far that focused on critical penetration conditions of gel particles into porous media at Darcy scale. Meanwhile, the understanding of Darcy-scale behaviors is practically more important for gel treatment design in field applications. It is crucial in determining whether gel materials can penetrate a porous medium, and whether and under what conditions selective penetration of gel materials into target channeling zones can be achieved.

In this work, we carried out a series of coreflooding experiments in a wide range of particle size and permeability conditions. On the basis of the experimental studies, a methodology was developed to describe the critical penetration conditions with the concept of threshold penetration pressure. The repeatability of the method was validated. The results could help identify favorable conditions to achieve selective penetration and thus effective conformance treatments.

2. Experimental and methodology

2.1. Microgels

Microgels used in this study were obtained by grinding dry millimeter-sized preformed particle gels into different size categories. The gels were synthesized with monomers (acrylamide), crosslinkers (N, N′-methylenebisacrylamide), initiators (peroxyldisulfate), and other additives (Bai et al., 2007a). The microgels had a volumetric swelling ratio of 20 cm^3/cm^3 in synthetic formation brine (total dissolved solids = 27,500 ppm) of the Milne Point oilfield. The swelling ratio was tested at reservoir temperature (~71 °F; formation: NB sand of Schrader Bluff). The composition of the formation brine was shown in Table 1. The swelling ratio was defined as the ratio of swollen volume after absorbing water to the original volume of the gel. Microgel dispersions were prepared with the formation brine at ~71 °F with a dry gel concentration of 1 wt%. In the preparation process, desired amount of gel particles with required size was added into the brine. The dispersions were mixed for two days to allow full swelling of the gel particles in the brine. More information about the brine, microgels and other materials can be found in our recent publications (Zhao et al. 2021a, 2021b; Bai et al., 2007a).

2.2. Superpermeable sandpacks, channel models, and matrix models

Different models were used to investigate the penetration behavior of microgels in super-k channels and reservoir matrices. Sandpacks were used to mimic super-k channels present in reservoirs. Sands with different size ranges were used to prepare the sandpacks. Larger sands resulted in higher permeabilities of the sandpacks. The sands were tightly packed to prevent potential remobilization during experiments. The sands were mixed with brine in favor of uniform packing. Also, stainless steel screens were used at both ends of the models to prevent sand from being flushed out. The screens also acted as distributors to allow uniform injection/production profiles at the sand faces, rather than entering/exiting the cores only from a small region adjacent to the injection/production holes of the coreholder. The permeabilities were in the range of 60–221 darcies. Sandwich-like channel models were also used to mimic heterogeneous reservoirs containing super-k channels (Fig. 2) . A typical channel model consisted of two half-cylindrical cores (mimicking reservoir matrices) and a super-k channel between the core plugs. The channel was created by filling sand grains in the fracture space between the core plugs. Detailed preparation processes of the channel models could be found in Zhao et al. (2021b). The permeabilities of the channels were in the range of 79–228 darcies. Berea and Boise sandstone cores were used to mimic reservoir matrices with relatively low permeabilities (50–5000 md). The super-k channel permeabilities covered the possible range tested in field-scale history matching studies (Wang et al., 2021). The intact core and the matrix permeabilities covered the varying permeabilities of the multilayer reservoir in Milne Point oilfield (Dandekar et al., 2019). Key information of the experiments was summarized in Table 2. For the channel models, the parameters (K, pore size, particle/pore ratio) pertained to the super-k channels. The average pore sizes were estimated with modified Carman-Kozeny equation (Zhao et al., 2021b). The particle/pore ratios in different experiments were also listed in the table.

2.3. Experiment setup and procedures

The experiment setup was shown in Fig. 3. The super-k sandpack models had three internal pressure taps (Fig. 3). The intact cores and the channel models did not have internal pressure taps. The multiple pressure sensors were able to monitor pressures at different locations in the sandpacks. The pressure sensors had fine sensitivity (0.001 psi) to

Table 1
Brine composition.

Name	Properties	Composition (ppm)
Synthetic formation brine	TDS = 27,500 ppm Ionic strength = 0.492 Hardness: 1700 ppm	Na^+: 10086.0 K^+: 80.2 Ca^{2+}: 218.5 Mg^{2+}: 281.6 Cl^-: 16834.4

Fig. 2. Photo of sandwich-like channel model. The model consisted of two semi-cylindrical cores (mimicking reservoir matrices) and a sand-filled high-permeability channel between the cores.

Table 2
Summary of basic information of the experiments.

Number	Model type	K, darcy	Dry gel particle size, mesh	Average swollen particle size D_g, µm	Average pore size D_p, µm	Particle/pore size ratio
1	Super-k sandpack	221	230/400	150	218.90	0.69
2	Super-k sandpack	62	230/400	130	116.81	1.11
3	Super-k sandpack	62.4	230/400	150	117.18	1.28
4	Super-k sandpack	60	230/400	150	114.84	1.31
5	Super-k sandpack	59.8	170/230	205	115.51	1.77
6	Intact core	4.74	230/400	136	33.74	4.03
7	Intact core	4.00	170/230	205	31.18	6.57
8	Intact core	4.28	120/170	290	32.12	9.03
9	Intact core	0.70	230/400	136	14.35	9.48
10	Intact core	0.44	170/230	205	11.77	17.41
11	Intact core	0.69	120/170	290	14.18	20.46
12	Intact core	0.37	120/170	290	10.77	26.93
13	Intact core	0.091	170/230	205	6.01	34.13
14	Intact core	0.052	120/170	290	4.53	64.04
15	Channel model	228	230/400	136	206.11	0.66
16	Channel model	221	230/400	136	203.12	0.67
17	Channel model	87	230/400	136	127.57	1.07
18	Channel model	179	170/230	205	181.86	1.13
19	Channel model	139	170/230	205	161.11	1.27
20	Channel model	218	120/170	290	202.31	1.43
21	Channel model	212	120/170	290	200.32	1.45
22	Channel model	79	170/230	205	121.55	1.69

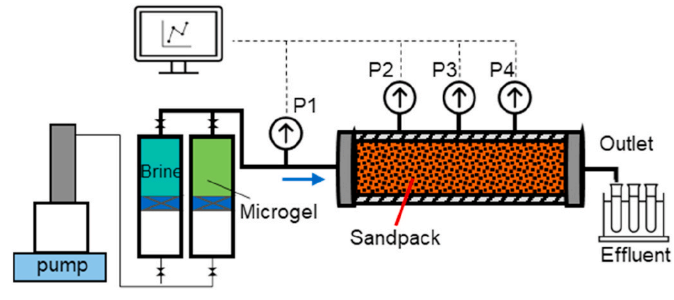

Fig. 3. Experiment setup for microgel transport tests.

capture detailed pressure responses during gel injection. The pressure sensor at the inlet was mounted as close as possible to the sand face and a large size (¼-in) swagelok tubing was used as the injection line. The designs minimized the pressure drop in the flowline. Data was logged at sufficient frequency (1 record/s) to capture the pressure responses during gel injection. An accumulator equipped with a mixing propeller at the bottom was used to store the gel dispersion. In this way, the gel particles could be uniformly dispersed in the carrying fluid while being injected into the core models.

The general experimental procedures included: (1) preparation of sandpack/core models, (2) injection of brine to test the water permeability at different flowrates, and (3) injection of gel dispersions at constant flow rates, except in Exp #1, #2, and #3, in which the gel dispersions were injected in constant-pressure mode. In experiments using superpermeable sandpack models and intact cores (except for Exp #1, #2, and #3), the superficial injection velocity was about 20 ft/d, and it was around 35 ft/d in experiments using channel models. Microgel dispersions were injected until stable pressures were established at all the pressure taps. The pressure responses were an indicator of gel transport in the cores. The time when the pressures at different locations began to increase was recorded. The onset of pressure increase indicated the microgel bank front arrived at the corresponding pressure taps.

3. Results and discussion

3.1. The threshold penetration pressures

Microgel dispersions were injected into super-k sandpacks to test the critical penetration behavior of microgels. Exp #4 was taken as an example to show how the threshold penetration pressures of microgel particles were determined. In this experiment, the gel dispersion was injected at constant flow rate of 2 ml/min (19.3 ft/d). The average particle/pore ratio was 1.31. The pressure responses at different locations were shown in Fig. 4. Obviously, the pressure at the inlet (P1) increased immediately as gel dispersion was injected into the model. Meanwhile, the pressure readings at the other locations (P2, P3 and P4) showed no increase. As gel dispersion was continuously injected, the other pressure sensors responded sequentially as gel particles transported to the corresponding pressure taps. Gels began to produce out from the outlet as more gel dispersion was injected, and the pressures at different locations gradually became relatively stable. Fig. 4 also showed a comparison of the pressure responses in the sandpack model (channel) and the intact core model (reservoir matrix). Obviously, with the increase of particle/pore size ratio, higher pressures were required to force the gel particles into the porous media.

3.1.1. Determination of the threshold penetration pressures

A close examine of the pressure response revealed that the pressures (P1 to P4) increased monotonically at the beginning (Fig. 5). When exceeding certain values (e.g., 5.02 psi for P1 in this experiment), the pressures began to exhibit obvious fluctuations. It is meaningful to link

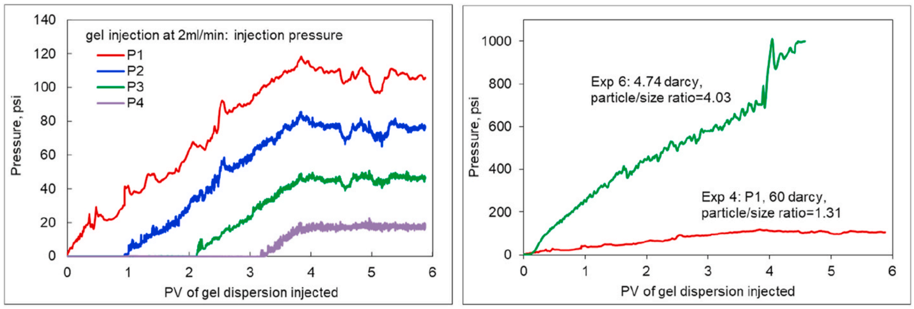

(a) Pressure responses at different locations (Exp #4). **(b) Comparison of pressure responses in Exp #4 and Exp #6**

Fig. 4. Pressure responses in Exp #4 and Exp #6.

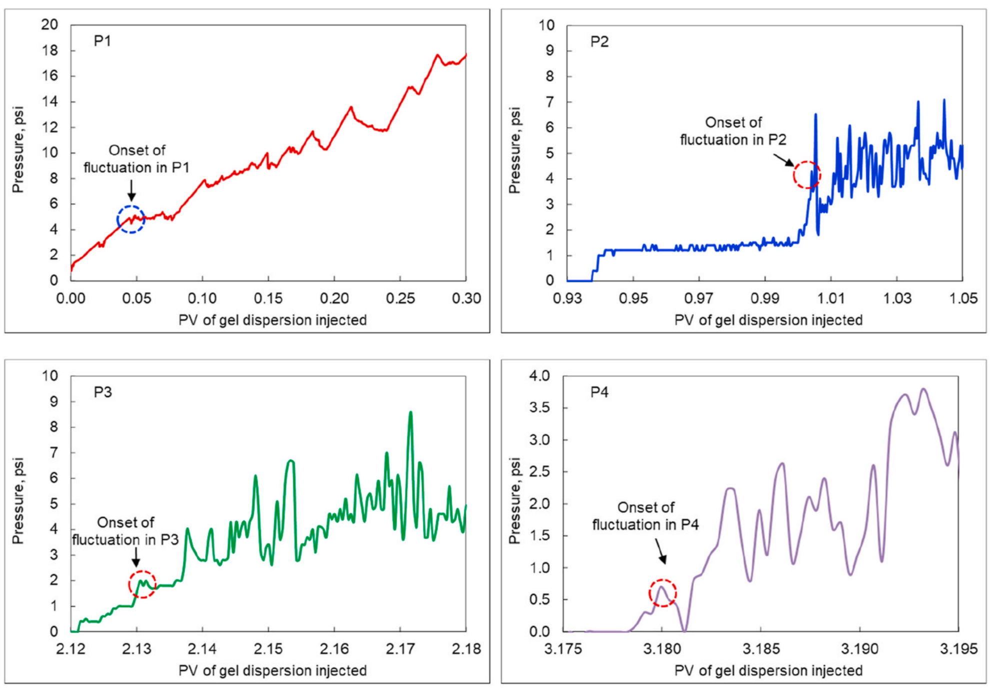

Fig. 5. Threshold penetration pressures at different locations indicated by the onset of pressure fluctuation (Exp #4).

the gel penetration/migration behaviors with the pressure responses. The pressure fluctuation is a macroscopic reflection of the viscoelastic nature of particulate materials propagating in porous media. It was caused by repeated accumulation and release (also called remigration) of gel particles at pore throats. When releasing, gel particles could be diverted to new channels and result in pressure fluctuations.

After the beginning of gel injection, the injection pressure increased and would exceed a certain value after some time. At this point, a significant portion of gel particles stuck at the pore throats began to remigrate (remobilize) and pass through the narrowest spots of pore throat structures. When looking at individual particles, some particles (especially the small ones) may have already penetrated the pores (especially the large ones) by a distance of several pore diameters. However, the Darcy-scale phenomenon (e.g., pressure fluctuation) was a statistic average effect of pore-scale processes, rather than a reflection of individual particle behavior. The onset of pressure fluctuations was associated with the critical state of particles beginning to remigrate (occurred at the narrowest spots within a distance of one to several pore diameters at the entrance). This status was regarded as the critical penetration condition of gel particles into porous media. The pressure was defined as the threshold penetration pressure (ΔP_{th}) accordingly. The threshold pressure was a practical Darcy-scale concept rather than a rigorous quantification of individual particles. It means, from an average macroscopic point of view, gel particles start to enter the porous media when the driving pressure exceeded the threshold value. Note that there are still knowledge gaps between the processes at different scales. Future work is required to further elucidate the connections between the processes at Darcy and pore scales. Fig. 5 shows the onsets of pressure fluctuations and the corresponding threshold penetration pressures at different locations in Exp #4.

3.1.2. *Lower ΔP_{th} inside the porous channels*

The ΔP_{th} showed a decreasing trend as the microgel particles transported deeper into the porous medium (Fig. 5). The trend was more evident as shown in Fig. 6. The threshold pressures at the four different locations were 5.02 psi, 4.30 psi, 2.00 psi and 0.70 psi, respectively. The inside average ΔP_{th} was 2.33 psi, which was lower than the value at the inlet face (5.02 psi). Similarly, the inlet threshold pressures and the inside average values in the other four experiments using super-k sandpacks were obtained. Fig. 7 plots the threshold pressures as a function of the particle/pore ratio. The inside threshold pressures were obtained by averaging the threshold pressures monitored at P2, P3 and

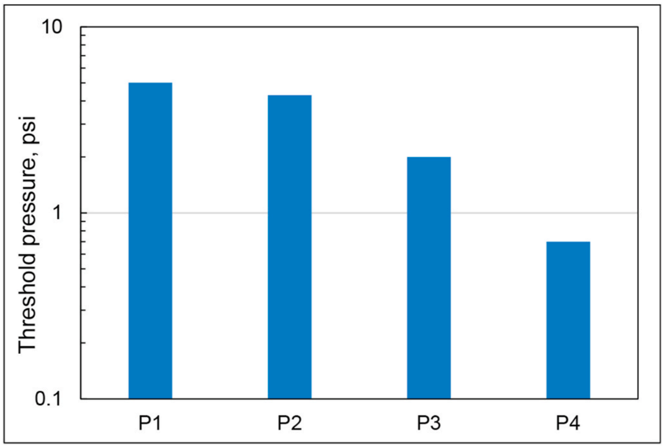

Fig. 6. Threshold penetration pressures at different transport distance (Exp #4).

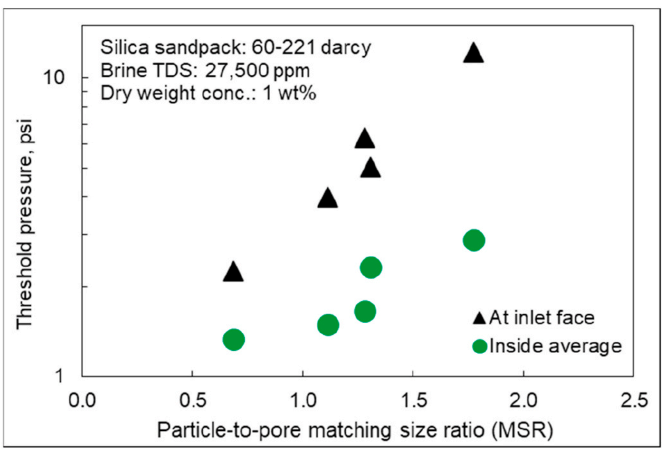

Fig. 7. Threshold penetration pressures at different particle/pore ratios.

P4. Generally, the threshold pressure exhibited a decreasing trend as the particles transporting deeper into the porous media. This was probably due to breakage of the particles under the shearing effect. The particles would break into smaller particles as they transported through the porous media especially at high flow rates. Another possible reason was adaptive behavior of the particles when transporting in the porous media. At the very beginning before entering the porous media, the particles had their original shape. Once entering the pore spaces, the viscoelasticity property made the particles adapt their geometry to the configuration of the pore-throat structures (A Newtonian fluid, e.g., water, could completely adapt to the flow pathways.). As a result, the axial dimension (in the migration direction) was increased, while the radial dimension was reduced. Thus, the gel particles were trained by the flow pathways to have a shape like an amoeba and wormhole through the porous media. Consequently, the resistances against the migration of the particle were reduced. Gel dehydration and gel filtration effect were also possible mechanisms that responsible for the decreasing threshold pressure. Future studies, such as visualization studies of gel injection through transparent small-size (centimeters or smaller) reservoirs, are required to justify the mechanisms and reveal the mysteries of soft particles transport through porous media. Fig. 7 also suggested that the threshold pressure increased with the particle/pore ratio (with one outlier). That is, higher threshold pressures were required to drive larger gel particles to penetrate the porous channels. The impact of particle/pore ratio was further studied in subsequent sections.

3.1.3. Threshold penetration pressures in homogeneous cores and channel models

For the intact core models, which simulated the matrices in reservoirs, the gel particles were very large relative to the pore throats (particle/pore ratio>4). High threshold penetration pressures were required as shown in Fig. 8. The gels were difficult in entering the cores. Instead, the gels accumulated at the inlet surfaces, and a gel cake was gradually formed (see Fig. 9 as an example). The cake further prevented the gel particles from penetrating the cores. The low penetration into the matrices was desirable to avoid massive formation damage. For the channel models, as shown in Fig. 10, the gels could not enter the matrices due to the high threshold pressures. Similar as observed in the homogeneous core models, a gel cake formed at the inlet surfaces of the matrices. On the contrary, the gels could easily penetrate the channel due to the low threshold penetration pressure in the channel (5.0 psi). Consequently, the gels selectively entered and placed in the super-k channel. The selective penetration feature of the gels was favorable for successful gel treatments.

3.2. Impact of particle/pore size ratio

The aforementioned results indicate that the particle/pore ratio significantly influences the penetration behavior of gels into channels and reservoir matrices. It is important to figure out under what conditions the gels can selectively penetrate the super-k channels without massively invading the reservoir matrices. The threshold penetration pressures (at inlets) in different experiments were plotted against the particle/pore ratio, as shown in Fig. 11. Correlations were developed to describe the relationship between the ΔP_{th} and the particle/pore ratio. The super-k channels covered permeabilities in the range of 60–230 darcies. The particle/pore ratios ranged from 0.66 to 1.77 (Table 2). The core models (matrices) covered permeabilities in the range of 50–5000 md. The particle/pore ratios ranged from 4.03 to 64.04. When the particle/pore ratios were larger than 20 (Exp #11 to Exp #14), the threshold penetration pressures were higher than 1200 psi.

3.2.1. Low ΔP_{th} in super-k channels

Fig. 11 elucidates the impact of matching size ratio on the threshold penetration pressure. In super-k channels, the particle/pore ratios are relatively low (<2). The threshold pressures are generally below 15 psi. The threshold pressure follows an exponential relationship with the particle/pore ratio. Their relationship can be described quite well with Eq. (1). In the equation (as well as in Eq. (2)), R_r was the average particle/pore ratio in the porous channels or reservoir matrices. For a given

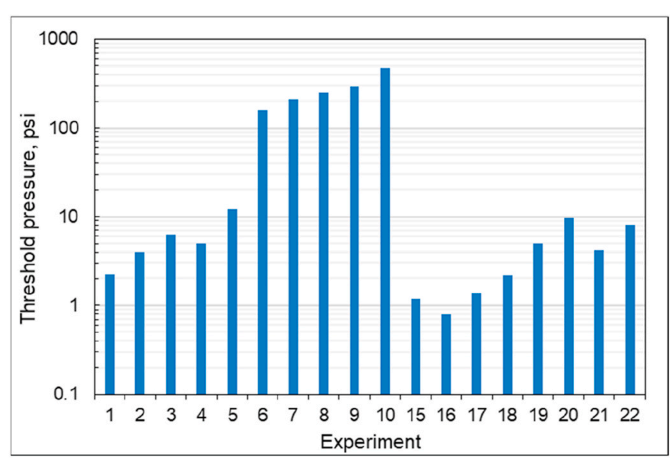

Fig. 8. Summary of threshold pressures in different experiments. (In Exps. #11 to #14, the values were higher than 1200 psi. However, no accurate threshold pressures were detected because the injection pressure exceeded the preset equipment limit.)

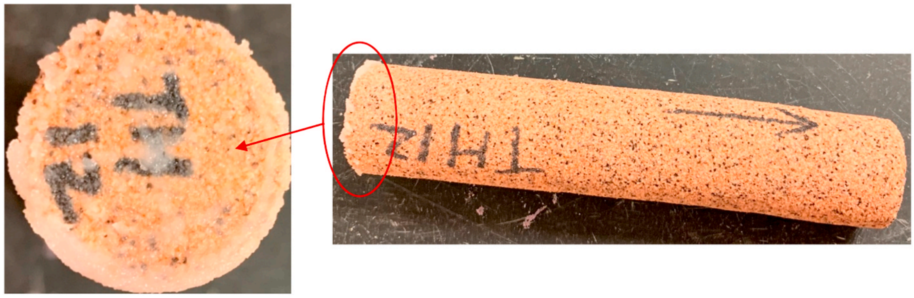

Fig. 9. A gel cake was formed at the inlet surface of an intact core (Exp #11, 693 md, particle/pore ratio = 20.46). (Due to the large gel sizes relative to the throats, a high threshold pressure, >1200 psi, was required to drive the gels to invade the core. The gel particles accumulated at the inlet surface, and a cake was gradually formed. The cake further prevented gel particles from entering the core.)

Fig. 10. A gel cake formed at the inlet surface of a channel model (Exp #19, 139 darcies, particle/pore ratio = 1.27, matrices 167 md). [Due to the high threshold pressure at the inlet surface of the matrices, a cake formed and further prevented the gels from invading the matrices. On the other hand, the low threshold pressure in the channel (5.0 psi) allowed easy penetration of the gels into the channel. As a result, the microgels selectively penetrated and placed in the super-k channel. After the gel treatment, the cake could be removed by soaking with chemical breakers to resume the injectivity of in the matrices. Selective penetration behavior was also observed in microgel treatment experiments in polymer flooding (Zhao et al., 2021b).].

particle gel system, the matching relationship of the threshold pressure and the permeability of the channel can be easily estimated. Thus, the threshold penetration pressure in the target channel can be evaluated with the correlation (Eq. (1)).

$$\Delta P_{th} = 0.305 \exp(2.0653 R_r),\ R_r < 3 \quad (1)$$

3.2.2. High ΔP_{th} in reservoir matrices

In the matrices, the particle/pore ratios are relatively high (>3). As shown in Fig. 11, the threshold pressures are higher than 100 psi. The threshold pressure also exponentially increases with the particle/pore ratio, but the increase is much more moderate compared with the situations in the super-k channels, as indicated by the slopes of the two fitting curves (2.0653 vs. 0.0785). The relationship between ΔP_{th} and particle/pore ratio can be described with Eq. (2) when the particle/pore ratio ranges from 3 to 20. The high penetration pressures make it hard for the gels to penetrate the reservoir matrices, which is favorable for effective gel treatments. Deviation curves were plotted against the trend lines in Fig. 11. As seen in the figure, all the experimental data points fell within the ±10% deviation curves when MSR≥3, and most data points (with three outliers) fell within the ±20% deviation curves when MSR<3. The results demonstrated the accuracy of the correlations in predicting the experimental data. The results also suggested good repeatability of the experimental observations.

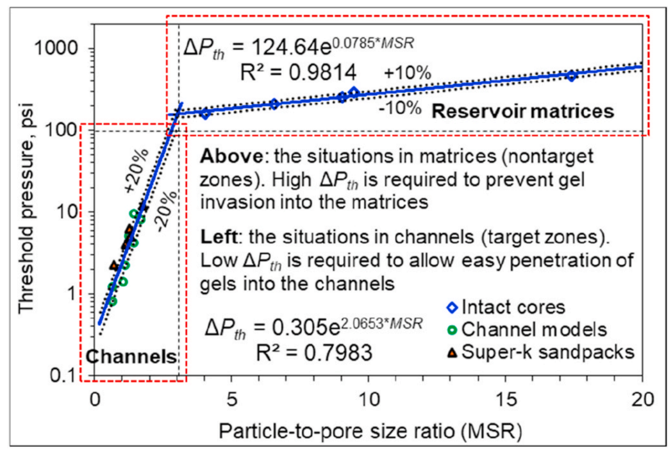

Fig. 11. Relationship between the threshold penetration pressure and the particle/pore size ratio.

$$\Delta P_{th} = 124.64 \exp(0.0785 R_r),\ 3 \le R_r < 20 \quad (2)$$

Interestingly, a distinct transition of the threshold pressure is identified at the particle/pore ratio of about 3. The particular behavior is closely related to the penetration and retention mechanisms of the elastic gel particles in porous channels and matrices. The flow paths in the porous media consisted of a series of convergent-divergent structures (i.e., pore throats). At high particle/pore ratios (e.g., particle/pore ratio>3 in this study), direct trapping of the gel particles at the pore throats would be dominant (Bai et al., 2007b; Yao et al., 2012). The gel particles should be deformed, dehydrated, and compressed, or/and even split into smaller pieces in order to pass through the pore throats. Under these conditions, the required driving pressures would be too high and break the particles into smaller pieces. Thus, the threshold penetration pressure would become less sensitive to the particle/pore ratio. Besides, at relatively high particle/pore ratios, the amoeba effect (Wang et al., 2015) mentioned in previous subsection can make the axial size of gel particles significantly larger than the radial size. The particles would adapt to and wormhole through the flow pathways. Therefore, the amoeba effect can also make the threshold pressure less sensitive to the gel size. It should be noted that some factors may influence the specific value of the transition point (particle/pore ratio≈3 in this work). It may change with the strength and concentration of the gel particles. Interestingly, Wang et al. (2017) also reported that particle breakage occurred when the particle/throat size ratio was larger than 3 for gel particles with different strengths. The transition point (when the breakage occurs) seems independent to the strength of the gel particles. Note that our experiment conditions (cores/sandpacks, gel particle suspensions) were substantially different with Wang et al. (2017) (single particle, single capillary tube). More work can be performed in the future to testify whether it is simply a coincidence or a universal behavior at different conditions. We did not have data points around MSR of 3 because of practical considerations in the experiment design. For channels to be treated, a matching size ratio above 2 was too large to achieve in-depth penetration of gel particles. For reservoir matrices, a size ratio below 5 was too low and would result in significant formation damage. Matching size ratios around 3 should be avoided for both the channels and the matrices in gel treatments.

The results reveal the underlying mechanism of selective penetration. In the matrices, due to the high threshold penetration pressures (Fig. 11), gel particles are difficult to penetrate the porous media. Instead, the gels accumulate at the inlet surface, and a gel cake is formed (Figs. 9 and 10). The cake further prevents the gels from entering the porous media. On the other hand, the gels can easily penetrate the super-k channels due to low threshold pressures (Fig. 11). According to the relationship between the threshold penetration pressure and the matching size ratio, favorable working conditions can be determined for effective gel treatments. The particle/pore ratio in the channel should be smaller than 2 to allow easy penetration into the target zones to be treated. Meanwhile, the particle/pore ratio in the matrix should be high enough to possess a high ΔP_{th} and thus prevent massive invasion into the matrix. For the tested microgels, an particle/pore ratio larger than 20 can substantially suppress gel invasion into reservoir matrices.

3.3. Further discussion

3.3.1. Impact of injection parameters (flow rate)

Higher flow rates result in larger driving forces. Gel particles are more likely to pass through the pore throat structures, and the gel retention (entrapment) would be lower as discussed by Farasat et al. (2017). However, the gel particles still need to overcome the maximum resistance in order to penetrate the rocks. For individual particles, the maximum resistance occurs at the narrowest spot (throat) of a pore-throat flow channel. It is a function of matching size ratio, particle strength, gel swelling/dehydration properties, dispersion concentration, and pore surface properties. Therefore, flow rate is not expected to significantly affect the threshold pressure. However, one possibility is that, at high flow rates, gel particles are more likely to break into smaller pieces, as observed in our previous paper (Zhao and Bai, 2021). In this way, the broken particles would need lower penetration pressures when transporting deeper into the rocks. Another consideration is the effect of inter-particle interactions at different flow rates. At this point, there is no clear clue about how flow rate impacts the interactions and thus the penetration pressure. The role of inter-particle interactions requires future investigations.

3.3.2. Impact of particle strength (elasticity) and dispersion concentration

Gel strength obviously affects the penetration pressure. It is not surprising stronger particles result in higher penetration pressures. Crosslinking density and gel structure influence the swelling property and strength of gels. Gel materials are usually stronger and more rigid with increased crosslinking density. Meanwhile, the swelling capacity is lower as less water can be absorbed. Dispersion concentration also affects the threshold pressure. As the concentration increases, inter-particle interactions become stronger. The gel particles are more likely to clog at pore throats. Accordingly, the threshold pressure will increase.

At current stage, our work was focused on the effect of matching size relationship. As more experimental data is available in the future, more robust and universal correlations can be developed to characterize the critical penetration behavior of such swellable particles into porous media.

3.3.3. Penetration pressure of different gels systems

The penetration pressure is expected to be very high for the cases of preformed bulk gels and in-situ formed gels. The high pressure means the gels are hard to be injected into formations. Seright (1999) tried to inject a preformed bulk gel [5000-ppm Cr(III)-acetate-HPAM] into a 28-darcy sandpack. A high pressure gradient (>200 psi/ft) was required to force the gel to propagate in the sandpack. The unsatisfactory injectivity is one drawback of the preformed bulk gel systems in dealing with such porous-medium-type channels. However, it is effective to seal off open fracture systems (Seright, 1997; Seright and Brattekas, 2021). For in-situ gel systems, a water-/polymer-solution-like gelant is initially injected into reservoirs to be treated. The gelant can significantly invade the reservoir matrices to cause damage if no additional measures are taken (e.g., zonal isolation), which is a drawback of such gel systems. Once the crosslinking reaction (namely gelation) takes place and gel networks form, the gel is hard to propagate farther. This feature is desirable because the gel can be held firmly in desired places.

4. Conclusions

This study investigated the critical penetration behavior of micrometer-sized preformed particle gels (microgel) into super-permeable (super-k) channels and matrices in a wide permeability range (50 md to 230 darcies). The results demonstrated the presence of threshold penetration pressure (ΔP_{th}), which was responsible for the selective penetration behavior of the tested microgels in channels and matrices.

(1) The critical penetration behavior was closely related to the particle/pore size ratio. The ΔP_{th} at the inlet faces of super-k channels (60–230 darcies) was in the range of 1–12 psi with particle/pore ratios in the range of 0.6–1.8. The low ΔP_{th} was beneficial to allow easy penetration of gel materials into the channeling zones.
(2) On the contrary, the ΔP_{th} was much higher in cores with relatively low permeabilities and high particle/pore ratios (ΔP_{th}>200 psi when the particle/pore ratio>6.5 for the tested gels). The high ΔP_{th} was desirable to prevent the gel materials from massively invading and damaging the matrices. Instead, the gel particles accumulated at the inlet surface, and a gel cake was gradually formed. The cake further prevented the invasion of gels into the matrices.
(3) Correlations were developed to describe the relationship between the ΔP_{th} and particle/pore ratio. When the particle/pore ratio<3, the ΔP_{th} exponentially increased with the particle/pore ratio. When the particle/pore ratio>3, the ΔP_{th} became much less sensitive to the particle/pore ratio, but it still exponentially increased with the particle/pore ratio. When the particle/pore ratio>20, the ΔP_{th} was higher than 1200 psi.
(4) This study provided quantitative evidence to demonstrate the selective penetration behavior of microgels. In addition, the concept of ΔP_{th} was utilized to figure out the favorable working conditions to achieve effective gel treatments. The particle/pore ratio in the channel should be sufficiently low to allow easy penetration of the gels into the channel (e.g., particle/pore ratio<2 in this study). Meanwhile, the particle/pore ratio in the matrix should be high enough to support a high ΔP_{th} and thus prevent massive invasion into the matrices.

Credit author statement

Yang Zhao: Conceptualization, Methodology, Investigation, Formal

Analysis, Data curation, Writing- Original draft preparation, Writing-Reviewing and Editing. **Baojun Bai**: Funding acquisition, Supervision, Resources, Conceptualization, Writing- Reviewing and Editing.

Declaration of competing interest

The authors confirm that there is no interest conflict.

Acknowledgement

The financial support from Department of Energy of the United States and Hilcorp Alaska (Award Number DE-FE0031606) was appreciated. This material is based upon work supported by the Department of Energy under Award Number DE-FE0031606. We appreciate the helpful comments from the reviewers and editors.

References

Bai, B., Huang, F., Liu, Y., Seright, R.S., Wang, Y., 2008. Case study on preformed particle gel for in-depth fluid diversion. In: Paper Presented at the SPE Symposium on Improved Oil Recovery, Tulsa, Oklahoma, USA. https://doi.org/10.2118/113997-MS. SPE-113997-MS.

Bai, B., Leng, J., Wei, M., 2021. A comprehensive review of in-situ polymer gel simulation for conformance control. Petrol. Sci. https://doi.org/10.1016/j.petsci.2021.09.041 (in press).

Bai, B., Li, L., Liu, Y., Liu, H., Wang, Z., You, C., 2007a. Preformed particle gel for conformance control: factors affecting its properties and applications. SPE Reservoir Eval. Eng. 10 (4), 415–421. https://doi.org/10.2118/89389-PA. SPE-89389-PA.

Bai, B., Liu, Y., Coste, J.P., Li, L., 2007b. Preformed particle gel for conformance control: transport mechanism through porous media. SPE Reservoir Eval. Eng. 10 (2), 176–184. https://doi.org/10.2118/89468-PA. SPE-89468-PA.

Bai, B., Wei, M., Liu, Y., 2012. Injecting large volumes of preformed particle gel for water conformance control. Oil Gas Sci. Technol. Rev. IFP Energies Nouvel. 67 (6), 941–952. https://doi.org/10.2516/ogst/2012058.

Bai, B., Wei, M., Liu, Y., 2013. Field and lab experience with a successful preformed particle gel conformance control technology. In: Paper Presented at the SPE Production and Operations Symposium, Oklahoma City, Oklahoma, USA, 23–26 March. https://doi.org/10.2118/164511-MS. SPE-164511-MS.

Choi, S.K., Sharma, M.M., Bryant, S.L., Huh, C., 2013. pH-sensitive polymers for novel conformance control and polymer flooding applications. SPE Reservoir Eval. Eng. 13 (6), 926–939.

Dandekar, A., Bai, B., Barnes, J., Cercone, D., Ciferno, J., Ning, S., Seright, R., Sheets, B., Wang, D., Zhang, Y., 2019. First ever polymer flood field pilot—a game changer to enhance the recovery of heavy oils on Alaska's North Slope. In: Paper Presented at the SPE Western Regional Meeting, San Jose, California, USA, 23–26 April. https://doi.org/10.2118/195257-MS. SPE-195257-MS.

Dandekar, A., Bai, B., Barnes, J., Cercone, D., Ciferno, J., Edwards, R., Ning, S., Schulpen, W., Seright, R., Sheets, B., Wang, D., Zhang, Y., 2020. First ever polymer flood field pilot to enhance the recovery of heavy oils on Alaska's North Slope–pushing ahead one year later. In: SPE Western Regional Meeting, April 27-30, 2020, Bakersfield, California, USA. Note – Postponed to Virtual Format in April 2021. SPE-200814-MS. https://doi.org/10.2118/200814-MS.

Dandekar, A., Bai, B., Barnes, J., Cercone, D., Ciferno, J., Edwards, R., Ning, S., Schulpen, W., Seright, R., Sheets, B., Wang, D., Zhang, Y., 2021. Heavy oil polymer EOR in the challenging Alaskan Arctic–it works!. In: Paper Prepared for Presentation at the Unconventional Resources Technology Conference Held in Houston, Texas, USA, 26-28 July 2021. URTeC-2021-5077. https://doi.org/10.15530/urtec-2021-5077.

Esfahlan, S.M., Khodapanah, E., Tabatabaei-Nezhad, S.A., 2021. Comprehensive review on the research and field application of preformed particle gel conformance control technology. J. Petrol. Sci. Eng. 2021 (202), 108440. https://doi.org/10.1016/j.petrol.2021.108440.

Farasat, A., Sefti, M.V., Sadeghnejad, S., Saghafi, H.R., 2017. Mechanical entrapment analysis of enhanced preformed particle gels (PPGs) in mature reservoirs. J Pet Sci Eng 157, 441–450. https://doi.org/10.1016/j.petrol.2017.07.028.

Farasat, A., Younesian-Farid, H., Sadeghnejad, S., 2021. Conformance control study of preformed particle gels (ppgs) in mature waterflooded reservoirs: numerical and experimental investigations. J. Petrol. Sci. Eng. (3–4), 108575. https://doi.org/10.1016/j.petrol.2021.108575.

Hendrickson, G.R., Lyon, L.A., 2010. Microgel translocation through pores under confinement. Angew. Chem. Int. Ed. 49, 2193–2197. https://doi.org/10.1002/anie.200906606.

Kang, W., Kang, X., Lashari, Z.A., Li, Z., Zhou, B., Yang, H., Sarsenbekuly, B., Aidarova, S., 2021. Progress of polymer gels for conformance control in oilfield. Adv. Colloid Interface Sci. 289 (March), 102363. https://doi.org/10.1016/j.cis.2021.102363.

Koochakzadeh, A., Younesian-Farid, H., Sadeghnejad, S., 2021. Acid pre-flushing evaluation before pH-sensitive microgel treatment in carbonate reservoirs: experimental and numerical approach. Fuel 297 (2), 120670.

Lalehrokh, F., Bryant, S.L., 2009. Application of pH-triggered polymers for deep conformance control in fractured reservoirs. In: Paper Presented at the SPE Annual Technical Conference and Exhibition, New Orleans, Louisiana. https://doi.org/10.2118/124773-MS. SPE-124773-MS.

Lei, W., Xie, C., Wu, T., Wu, X., Wang, M., 2019. Transport mechanism of deformable micro-gel particle through micropores with mechanical properties characterized by AFM. Sci. Rep. 9, 1–12. https://doi.org/10.1038/s41598-018-37270-7.

Leng, J., Wei, M., Bai, B., 2021. Review of transport mechanisms and numerical simulation studies of preformed particle gel for conformance control. J. Petrol. Sci. Eng. 206 (November), 109051. https://doi.org/10.1016/j.petrol.2021.109051.

Li, Y., Sarıyer, O.S., Ramachandran, A., Panyukov, S., Rubinstein, M., Kumacheva, E., 2015. Universal behavior of hydrogels confined to narrow capillaries. Sci. Rep. 5 (1) https://doi.org/10.1038/srep17017, 17017: 1-11.

Liu, Y., Hou, J., Wang, Q., Liu, J., Guo, L., Yuan, F., Zhou, K., 2017. Flow of preformed particle gel through porous media: a numerical simulation study based on the size exclusion theory. Ind. Eng. Chem. Res. 56, 2840–2850. https://doi.org/10.1021/acs.iecr.6b03656.

Mathur, B., Dandekar, A.Y., Khataniar, S., Patil, S.L., 2017. Life after CHOPS: alaskan heavy oil perspective. In: Paper Presented at the SPE Western Regional Meeting, Bakersfield, California. https://doi.org/10.2118/185704-MS. SPE-185704-MS.

Ning, S., Barnes, J., Edwards, R., Schulpen, W., Dandekar, A., Zhang, Y., Cercone, D., Ciferno, J., 2020. First ever polymer flood field pilot to enhance the recovery of heavy oils on Alaska North Slope–producer responses and operational lessons learned. In: Paper Presented at the SPE Annual Technical Conference and Exhibition, Virtual, 26–29 October. https://doi.org/10.2118/201279-MS. SPE-201279-MS.

Saghafi, H.R., Emadi, M.A., Farasat, A., Arabloo, M., Naderifar, A., 2016. Performance evaluation of optimized preformed particle gel (PPG) in porous media. Chem. Eng. Res. Des. 112, 175–189. https://doi.org/10.1016/j.cherd.2016.06.004.

Seright, R.S., 1997. Use of preformed gels for conformance control in fractured systems. SPE Prod. Facil. 12 (1), 59–65. https://doi.org/10.2118/35351-PA. SPE-35351-PA.

Seright, R.S., 1999. Mechanism for gel propagation through fractures. In: Paper Presented at the SPE Rocky Mountain Regional Meeting, Gillette, Wyoming, USA, 15–18 May. https://doi.org/10.2118/55628-MS. SPE-55628-MS.

Seright, R.S., Brattekas, B., 2021. Water shutoff and conformance improvement: an introduction. Petrol. Sci. 18, 450–478. https://doi.org/10.1007/s12182-021-00546-1.

Sydansk, R.D., Romero-Zeron, L., 2011. Reservoir Conformance Improvement. Society of Petroleum Engineers, Richardson, Texas, USA.

Teimouri, A., Sadeghnejad, S., Dehaghani, A.H.S., 2020. Investigation of acid pre-flushing and pH-sensitive microgel injection in fractured carbonate rocks for conformance control purposes. Oil Gas Sci. Technol. Rev. IFP Energies Nouvel. 75 (2), 52.

Villone, M.M., Maffettone, P.L., 2019. Dynamics, rheology, and applications of elastic deformable particle suspensions: a review. Rheol. Acta 58 (3–4), 109–130. https://doi.org/10.1007/s00397-019-01134-2.

Wang, J., Zhang, H., Liu, H., Zhao, W., Liu, H., Yao, C., Zheng, J., Shen, Y., 2017. Quantification of transportation of deformable gel particles in porous media. In: Paper Presented at the SPE Annual Technical Conference and Exhibition Held in San Antonio, Texas, USA, 9-11 October. https://doi.org/10.2118/187266-MS. SPE-187266-MS.

Wang, X., Keith, C., Zhang, Y., Dandekar, A., Ning, S., Wang, D., Edwards, R., Barnes, J., Girbacea, R., Cercone, D., Ciferno, J., 2021. History matching and performance prediction of a polymer flood pilot in heavy oil reservoir on Alaska North Slope. In: Paper Presented at the 2021 SPE Annual Technical Conference and Exhibition Held in Dubai, UAE, 21-23 September. https://doi.org/10.2118/206247-MS.

Wang, Y., Jin, J., Bai, B., Wei, M., 2015. Study of displacement efficiency and flow behavior of foamed gel in non-homogeneous porous media. PLoS One 10 (6), e0128414.

Yao, C., Lei, G., Cathles, L.M., Steenhuis, T.S., 2014. Pore-scale investigation of micron-size polyacrylamide elastic microspheres (MPEMs) transport and retention in saturated porous media. Environ. Sci. Technol. 48, 5329–5335. https://doi.org/10.1021/es500077s.

Yao, C., Lei, G., Li, L., Gao, X., 2012. Selectivity of pore-scale elastic microspheres as a novel profile control and oil displacement agent. Energ Fuel 26, 5092–5101. https://doi.org/10.1021/ef300689c.

Yao, C., Liu, B., Li, L., Zhang, K., Lei, G., Steenhuis, T.S., 2020. Transport and retention behaviors of deformable polyacrylamide microspheres in convergent-divergent microchannels. Environ. Sci. Technol. 54, 10876–10884. https://doi.org/10.1021/acs.est.0c02243.

Zhang, Z., Xu, J., Drapaca, C., 2018. Particle squeezing in narrow confinements. Microfluid. Nanofluidics 22, 1–26. https://doi.org/10.1007/s10404-018-2129-2.

Zhao, W., Liu, H., Wang, J., Zhang, H., Yao, C., Wang, L., Qi, P., 2018. Investigation of restarting pressure gradient for preformed particle gel passing through pore-throat. J. Petrol. Sci. Eng. 168, 72–80. https://doi.org/10.1016/j.petrol.2018.05.005.

Zhao, Y., Bai, B., 2021. Experimental study of transport behavior of swellable microgel particles in superpermeable channels for conformance control. SPE J. 2021. https://doi.org/10.2118/208576-PA. SPE-208576-PA.

Zhao, Y., Leng, J., Lin, B., Wei, M., Bai, B., 2021a. Experimental study of microgel conformance-control treatment for a polymer-flooding reservoir containing superpermeable channels. SPE J. 26 (4), 2305–2317. https://doi.org/10.2118/205486-PA. SPE-205486-PA, 2021.

Zhao, Y., Yin, S., Seright, R.S., Ning, S., Zhang, Y., Bai, B., 2021b. Enhancing heavy-oil-recovery efficiency by combining low-salinity-water and polymer flooding. SPE J. 26 (3), 1535–1551. https://doi.org/10.2118/204220-PA. SPE-204220-PA.

Zhou, K., Hou, J., Sun, Q., Guo, L., Bing, S., Du, Q., Yao, C., 2017. An efficient LBM-DEM simulation method for suspensions of deformable preformed particle gels. Chem. Eng. Sci. 167, 288–296. https://doi.org/10.1016/j.ces.2017.04.026.

Zhu, D., Bai, B., Hou, J., 2017. Polymer gel systems for water management in high-temperature petroleum reservoirs: a chemical review. Energy Fuels 2017 31 (12), 13063–13087.